

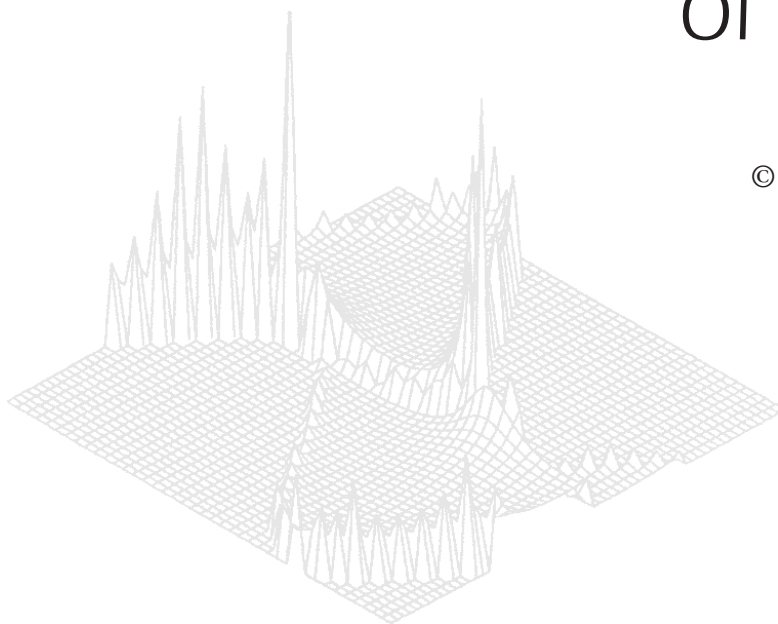
---

CSIRO PUBLISHING

---

# Australian Journal of Physics

Volume 50, 1997  
© CSIRO Australia 1997



A journal for the publication of  
original research in all branches of physics

[www.publish.csiro.au/journals/ajp](http://www.publish.csiro.au/journals/ajp)

All enquiries and manuscripts should be directed to

*Australian Journal of Physics*

**CSIRO PUBLISHING**

PO Box 1139 (150 Oxford St)

Collingwood

Vic. 3066

Australia

Telephone: 61 3 9662 7626

Facsimile: 61 3 9662 7611

Email: [peter.robertson@publish.csiro.au](mailto:peter.robertson@publish.csiro.au)



Published by **CSIRO PUBLISHING**  
for CSIRO Australia and  
the Australian Academy of Science



## Structure Functions of Hadrons in the QCD Effective Theory\*

*Takayuki Shigetani*,<sup>A</sup> *Katsuhiko Suzuki*<sup>B</sup> and *Hiroshi Toki*<sup>C</sup>

<sup>A</sup> Department of Physics, Tokyo Metropolitan University,  
Hachioji, Tokyo 192-03, Japan.  
email: shige@atlas.phys.metro-u.ac.jp

<sup>B</sup> Institut für Theoretische Physik,  
Technische Universität München, Germany.

<sup>C</sup> Research Centre for Nuclear Physics, Osaka University,  
Osaka, Japan.

### *Abstract*

We study the structure functions of hadrons with the low energy effective theory of QCD. We try to clarify a link between the low energy effective theory, where non-perturbative dynamics is essential, and the high energy deep inelastic scattering experiment. We calculate the leading twist matrix elements of the structure function at the low energy model scale within the effective theory. Calculated structure functions are taken to the high momentum scale with the help of the perturbative QCD, and compared with the experimental data. Through a comparison of the model calculations with the experiment, we discuss how the non-perturbative dynamics of the effective theory is reflected in the deep inelastic phenomena. We first evaluate the structure functions of the pseudoscalar mesons using the NJL model. The resulting structure functions show reasonable agreement with experiments. We then study the quark distribution functions of the nucleon using a covariant quark-diquark model. We calculate three leading twist distribution functions, the spin-independent  $f_1(x)$ , the longitudinal spin distribution  $g_1(x)$ , and the chiral-odd transversity spin distribution  $h_1(x)$ . The results for  $f_1(x)$  and  $g_1(x)$  turn out to be consistent with available experiments because of the strong spin-0 diquark correlation.

### **1. Introduction**

In the last several decades, the structure functions of hadrons have been extensively studied, and have provided us with detailed information on the internal structures of hadrons. The experiment in the high energy region, e.g. deep inelastic scattering of hadrons (DIS), is one of the most powerful tools to investigate the internal quark and gluon structure. Progress in the experimental technique makes it possible to investigate the details of the structure functions of hadrons, and to produce a large amount of data.

It is now generally accepted that the hadron is composed of quarks and gluons. Quantum chromodynamics (QCD) is believed to be a fundamental theory of the strong interaction, which describes hadrons and nuclei in terms of quarks and

\* Refereed paper based on a contribution to the Japan–Australia Workshop on Quarks, Hadrons and Nuclei held at the Institute for Theoretical Physics, University of Adelaide, in November 1995.

gluons. We can in principle obtain the properties of hadrons from QCD. However, QCD becomes non-perturbative at the low energy scale, because the coupling constant is very large and the perturbative treatment is not valid. Hence, it is very difficult to extract the low energy hadron properties from QCD. A simple and useful approach for the treatment of non-perturbative QCD is to construct a low energy effective model which contains the essential aspects of QCD. On the other hand, the coupling constant of QCD becomes small at the high energy scale, and hence the perturbative QCD (pQCD) becomes reliable. This behaviour is called asymptotic freedom, which is the most important aspect of QCD as a non-abelian gauge theory. In fact, the observed scaling violations of the structure functions are consistent with the perturbative QCD predictions. QCD, however, is not able to predict the structure function itself at the present.

It is of great interest to clarify a connection between the high energy experiments, especially DIS phenomena, and the low energy quark models. At the experimental large momentum scale, a virtual photon sees a hadron as a complicated object, which consists of valence quarks, sea quarks, and gluons. As the momentum scale becomes smaller, sea quarks and gluons are absorbed into valence quarks, and their degrees of freedom are substituted by the ‘constituent quarks’, whose dynamics is subject to the low energy QCD. If we relate the DIS data with the effective models, we can learn how the non-perturbative aspects of QCD reflect the behaviour of the quark distributions at the DIS energy scale. In fact, recent DIS experiments provide surprising discoveries which are beyond the scope of the perturbative QCD and may be due to the non-perturbative dynamics. Hence, it is crucial to study the connection between the deep inelastic phenomena and the non-perturbative low energy hadron physics by using the quark models. Such a connection would enable us to use the high energy experimental data to constrain the models of low energy QCD.

Indeed, theoretical studies for the structure functions of hadrons are made in terms of several effective quark models, which are supposed to work at the low energy scale. Those works are based on the assumption that the structure functions at the low energy model scale,  $Q^2 = Q_0^2$ , are obtained by calculating the twist-2 matrix elements within the effective models. In the formalism of the operator product expansion (OPE), the  $n$ th moment of the structure function  $F_2(x)$  at the scale  $Q^2$  is expanded as

$$\int dx x^{n-2} F_2(x, Q^2) = \sum_{\tau} C_{\tau}^n(Q^2, Q_0^2) \langle h | \mathcal{O}_{\tau}^n(Q_0^2) | h \rangle, \quad (1-1)$$

where  $C_{\tau}^n(Q^2, Q_0^2)$  are the Wilson coefficients calculated by the perturbative QCD, and  $\langle h | \mathcal{O}_{\tau}^n(Q_0^2) | h \rangle$  are the expectation values of the local operators which are evaluated at the arbitrary scale  $Q_0^2$ . Note that the Wilson coefficients are simple  $c$ -numbers, and the expectation values of the local operators depend only on  $Q_0^2$ . The perturbative QCD provides the Wilson coefficients, and thus predicts the momentum  $Q^2$ -dependence of the structure function. In order to get the matrix elements of local operators, however, it is necessary to construct the hadron state  $|h\rangle$ , which is governed by the non-perturbative QCD. Therefore, most of the works on DIS have been devoted to the calculation of the perturbative part (Wilson coefficients). The focus of this paper is, on the contrary, to make use of the

matrix elements which appear in the deep inelastic process to get information on the detailed hadron structure. In the Bjorken limit ( $Q^2 \rightarrow \infty$ ), only the twist-2 ( $\tau = 2$ ) term survives in eq. (1-1) and the higher twist terms become negligible [ $\sim O(1/Q^2)$ ]. Hence, once we calculate the twist-2 operators within the quark model at the low momentum scale  $Q_0^2$ , where the phenomenological model makes sense, we can get the structure function at the experimental scale  $Q^2$  using the QCD evolution equation. Thus, a comparison with experiments can be made.

In this talk, we first focus on the structure functions of mesons in terms of the Nambu and Jona-Lasinio (NJL) model. We next extend our study to the quark distribution functions of the nucleon using a covariant quark-diquark model. We calculate three leading twist distribution functions, which are the spin independent distribution  $f_1(x)$ , the longitudinal spin distribution  $g_1(x)$ , and the chiral-odd transversity spin distribution  $h_1(x)$ .

## 2. Meson Structure Function

### (2a) Calculation of Meson Structure Function

We first evaluate the structure functions of mesons,  $\pi$  and  $K$ , in terms of the Nambu and Jona-Lasinio (NJL) model, as done in ref. [1]. Although the available experimental data on the meson structure function are much fewer than that of the nucleon, the meson structure functions are also important in studying the quark structure of hadrons. Comparing with the nucleon case, one may extract more directly the information on the quark-quark interaction from the structure function, since we can avoid solving the complicated three body problem as the nucleon case.

In the NJL model, the gluon degrees of freedom are assumed to be frozen into a chiral invariant effective 4-point interaction in the low energy region. The NJL model demonstrates the spontaneous breakdown of chiral symmetry and the emergence of the Goldstone bosons. The generalized  $SU(3)_f$  NJL model reproduces the meson properties remarkably well, in spite of the lack of confinement. This model is also applied to the chiral phase transition at finite temperature and density. All these results indicate that the NJL model possesses the essential features of QCD.

The hadronic tensor is related to the forward scattering amplitude  $T_{\mu\nu}$  through the optical theorem  $W_{\mu\nu} = \frac{1}{2\pi} \text{Im}T_{\mu\nu}$ . Thus, we calculate  $T_{\mu\nu}$  in the NJL model to get the structure functions. We compute the forward scattering amplitude  $T_{\mu\nu}$  in the impulse approximation of the pseudoscalar meson case, which is illustrated as ‘handbag diagrams’. After calculations in the Bjorken limit [3, 1], we can obtain

$$\begin{aligned}
 T_{\mu\nu} = & \frac{8}{9} \frac{i}{(2\pi)^3} N_c g_{pq}^2 \int d\mu^2 \left[ \left( \frac{1}{(\mu^2 - M_1^2)} \right) - x \left( \frac{2M_1 M_2 - (M_1^2 + M_2^2) + p^2}{(\mu^2 - M_1^2)^2} \right) \right] \\
 & \times \theta(x(1-x)m_{ps}^2 - xM_2^2 - (1-x)\mu^2) \\
 & \times \left[ -g_{\mu\nu} + \frac{2z}{m_{ps}\nu} p_\mu p_\nu + \frac{1}{m_{ps}\nu} (p_\mu q_\nu + p_\nu q_\mu) \right], \quad (2-1)
 \end{aligned}$$

Here  $x$  is the so-called Bjorken  $x$ , and  $m_{ps}$  the pseudoscalar meson mass. Also  $M_1$  is the constituent mass of the struck quark, and  $M_2$  the mass of the spectator antiquark, which are solutions of the gap equation due to the dynamical chiral symmetry breaking. In the case of the pion, we set  $M_1 = M_2 = M_{u(d)}$ . For the  $K^+$  meson,  $M_1 = M_u$  and  $M_2 = M_S$ . It is easily seen from (2-1) that the calculated structure functions exhibit Bjorken scaling [4].

Taking the imaginary part in (2-1), we get the valence quark distribution of the pseudoscalar meson by the use of the optical theorem:

$$q(x) \propto -g_{pqq}^2 \int_{-\infty}^0 d\mu^2 \left[ \frac{1}{\mu^2 - M_1^2} - x \frac{2M_1M_2 - (M_1^2 + M_2^2) + p^2}{(\mu^2 - M_1^2)^2} \right] \times \theta(p^2x(1-x) - xM_2^2 - (1-x)\mu^2) \quad (2-2)$$

where  $p^2 = m_{ps}^2$ . We use the Euclidean variable  $\mu_E^2 = -\mu^2$  for the integration of (2-2) with the momentum cutoff. We introduce the Fermi-distribution type momentum cutoff function

$$\int d^4k \rightarrow i \int d^4k_E \frac{1}{1 + \exp[(k_E^2 - \Lambda^2)/a]}. \quad (2-3)$$

Here  $k_E^2$  is the Euclidean four momentum squared, and  $\Lambda$  is identified with the typical scale of the chiral symmetry breaking  $\sim 1$  GeV. We use  $a \sim 0.1$  GeV<sup>2</sup> to reproduce the meson properties.

Note that the resulting distribution shows the correct behaviour  $q(x) \rightarrow 0$  as  $x \rightarrow 1$ , since the lower limit of the integral  $\mu_{E \min}^2 (= -\mu_{\max}^2) = \frac{x}{1-x}M_2^2 - xp^2 \rightarrow \infty$  as  $x \rightarrow 1$  [4]. We also note that the contribution of the second term of (2-2) to the distribution function is small. This smallness is due to the spontaneous breakdown of chiral symmetry. In fact, the second term disappears in the chiral limit;  $m_u = m_d = m_s = 0$ . This form ensures the behaviour  $xq_{val}(x) \propto x$  at small  $x$ . If chiral symmetry were not spontaneously broken, the second term would be as large as the first term and the pionic quark distribution would behave  $xq(x)_{val} \propto x^2$  around small  $x$ .

### (2b) Numerical Results

We show numerical results for the quark distribution functions with the use of the parameters which are used in ref. [1]. We first show in Fig. 1 the quark distribution in the pion expressed as (2-2) by the dotted curve at the low energy model scale,  $Q = Q_0^2$ . The peak of the resulting distribution appears at  $x \sim 0.6$ , which indicates asymmetric momentum distributions in the pion; the struck quark carries a larger part of the pion momentum. This is due to the large binding energy of the valence quark in the pion. This result is a consequence of the highly non-perturbative structure of the pion.

We note that this low energy scale structure function has no physical meaning at this scale, since the ‘real’ structure function at the low energy scale receives non-negligible contributions from all twist operators. The contribution from leading twist, however, can survive at the high energy scale. The calculated results represented by the dotted curve in Fig. 1 do not depend on  $Q^2$  explicitly,

as they receive the logarithmic QCD radiative corrections. We use the first order Altarelli–Parisi equation [5] for the  $Q^2$  evolution of valence distributions with  $\Lambda_{QCD} = 250$  MeV to compare our results with experiment. We take the low energy hadronic scale at  $Q_0^2 = (0.5 \text{ GeV})^2$ , which is used in ref. [6].

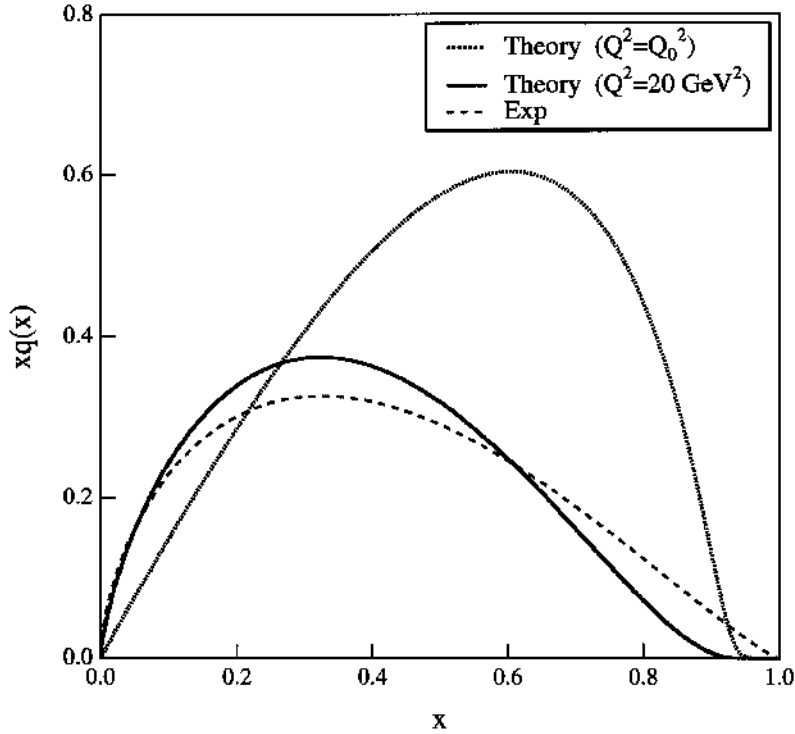


**Fig. 1.** Valence quark distribution of the pion at  $Q^2 = 20 \text{ GeV}^2$  (solid curve) as a function of the Bjorken  $x$ , in which we use the model scale  $Q_0^2 = 0.25 \text{ GeV}^2$ . The experimental fit [7] is depicted by the dashed curve.

We show the pionic quark distribution at  $Q^2 = 20 \text{ GeV}^2$  by the solid curve in Fig. 1 with experimental data (the dashed curve) extracted from the Drell–Yan process [7]. We find reasonable agreement with experiment. The second moment of the valence quark, which is identified with a momentum fraction carried by the valence quark, turns out to be,  $\langle xu \rangle_\pi = 0.22$  at  $Q^2 = 20 \text{ GeV}^2$ , where  $\langle xq \rangle = \int_0^1 dx xq(x)$ . This value is remarkably consistent with the experimental 0.21 [7]. However, the calculated distribution function is almost zero at  $x \sim 1$ , and different from the experimental fit [7] or the counting rule prediction [2]. This shortcoming comes from the cutoff procedure of the model. Around  $x \sim 1$ , the struck quark has a very large momentum  $> 1 \text{ GeV}$ , and the quarks with very large momenta are excluded in the NJL model by the cutoff. At the moment, such a high momentum quark cannot exist in the hadron wave function within the low energy quark model, and we need to develop a model to include the high momentum correlations consistently with the low energy theory.

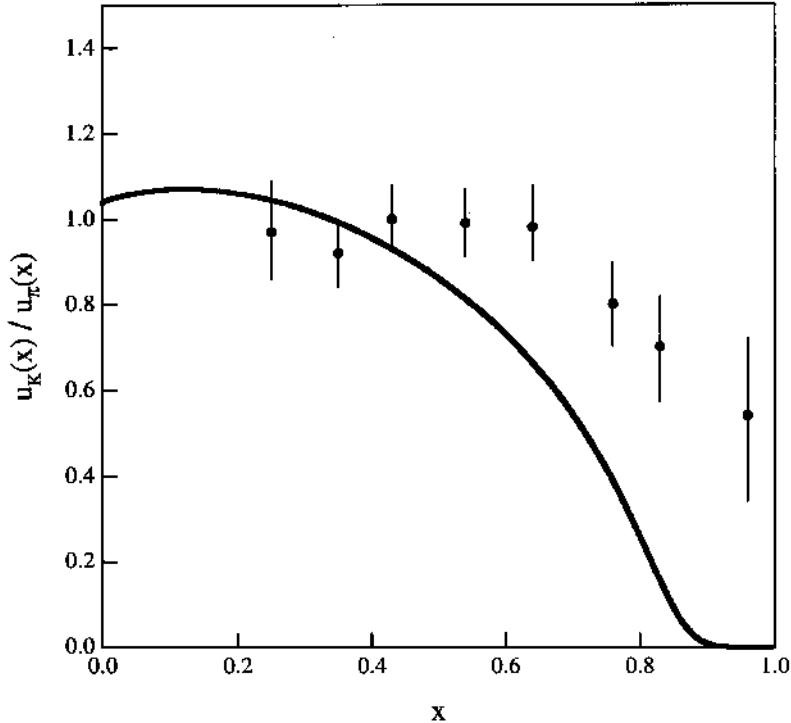


**Fig. 2.** Ratio of kaon to pion valence  $u$  quark distributions  $u_K(x)/u_\pi(x)$  at  $Q^2 = 20 \text{ GeV}^2$ . The theoretical result is depicted by the solid curve. The closed circles with error bars are taken from the Drell–Yan experiment [8].

The valence quark distribution of the kaon is also interesting. The corresponding second moments of the valence quarks in the kaon are given by  $\langle xu \rangle_K = 0.20$ ,  $\langle xs \rangle_K = 0.24$  at  $Q^2 = 20 \text{ GeV}^2$ . The result indicates that the heavy strange quark has a larger momentum in the kaon than the light  $u$ ( $d$ ) quark. The total momentum carried by the valence quarks in the kaon is  $\langle xu \rangle_K + \langle xs \rangle_K = 0.44$ , and is almost the same as that in the pion  $2\langle xu \rangle_\pi = 0.43$ . We also show in Fig. 2 the ratio of kaon to pion valence  $u$ -quark distributions  $u_K/u_\pi$  at  $Q^2 = 20 \text{ GeV}^2$ . The experimental values are taken from the Drell–Yan experiment [8]. The result is consistent with available experiments.

### 3. Nucleon Structure Function

In this section we study the quark distribution functions of the nucleon. Recent measurements of deep inelastic scattering show clear flavour dependence of the nucleon structure functions. One example is the ratio of the neutron to proton structure functions  $F_2^n(x)/F_2^p(x)$  which shows a large deviation from the naive quark–parton model prediction, which is  $2/3$ . On the other hand, the polarized structure function  $G_1^{p,n}(x)$  shows some deviation from the result of the naive quark–parton model,  $A_1^p = G_1^p(x)/F_1^p(x) = 5/9$  [9, 10, 11]. These results indicate that the parton model neglects correlations among partons. Hence, we shall discuss these problems within an effective model, which takes into account the quark correlations in the nucleon.

The quark distribution function of the nucleon in QCD can be defined by the light-cone Fourier transformation of products of operators between hadron states as discussed in [12]. We shall discuss the usual spin-independent quark distribution  $f_1(x)$ , the quark helicity distribution function in the longitudinally polarized nucleon  $g_1(x)$  and the *transversity* spin distribution function  $h_1(x)$ . We use the relativistic quark–diquark model for the nucleon for the calculation of these nucleon distribution functions. The idea of diquarks, i.e. correlated states of two quarks, is first introduced phenomenologically to explain the scaling violation of the nucleon structure functions, which may be caused by the non-perturbative diquark correlations [13].

The nucleon properties such as the mass and the wave function within the NJL model should be obtained by solving the relativistic three body problem, and such an effort is being made with the relativistic Faddeev method [14]. It seems, however, necessary to incorporate confinement for a successful description of baryons, which is absent in the NJL model. Therefore, we simply take the quark–diquark model for the nucleon, and assume the case of the diquark–quark vertex being scalar [15];

$$\Gamma_{Dq}(p^2) \propto \mathbf{1} \cdot \phi(p^2), \quad (3-1)$$

where  $\mathbf{1}$  is the unit matrix in the Dirac space.

First, we evaluate contributions of the diagram where a quark is struck out by the virtual photon with the residual diquark being a spectator. This part can be calculated following the work of Meyer and Mulders [15]. We use the impulse approximation, and thus the hadronic tensor is represented by an incoherent sum of various processes. We define the constituent quark mass  $m$  and the diquark mass  $m_D$  inside the nucleon, though the diquark and the quark are not the eigenstates of QCD. Their values are obtained within the NJL model.

The calculation of the hadronic tensor in the Bjorken limit yields the spin independent and dependent distribution functions [15]

$$q^D(x) = \int_{p_E^2 \min}^{\infty} \frac{dp_E^2}{8\pi^2} \frac{\phi^2(p_E^2)}{(p_E^2 + m^2)^2} [x(M^2 + 2mM - m_D^2) + m^2 + (1-x)p_E^2], \quad (3-2)$$

$$\begin{aligned} \delta^D(x) = \int_{p_E^2 \min}^{\infty} \frac{dp_E^2}{8\pi^2} \frac{\phi^2(p_E^2)}{(p_E^2 + m^2)^2} [2x^2M^2 - xM^2 \\ + 2mMx + m_D^2x + m^2 - (1-x)p_E^2], \quad (3-3) \end{aligned}$$

where

$$p_{E \min}^2 = \frac{x}{1-x} m_D^2 - xM^2,$$

and  $M$  is the nucleon mass. Here  $P$  is the proton momentum, and  $p$  and  $p_2$  are the momenta of the struck quark and the spectator diquark, respectively.

To avoid divergence in (3-2) and (3-3), we introduce the regularization function  $\phi(p_E^2)$  in Euclidean space, which is used in our calculation of the meson structure functions in the NJL model. We present here the calculated result

on the structure function. We use the NJL model parameters, which are fixed by the pion properties. For the diquark part, we treat the diquark masses as free parameters. By analysis of the N- $\Delta$  mass splitting in the one-gluon exchange picture, the scalar diquark mass  $m_S$  was assumed to be 585 MeV [16], and the axial-vector diquark mass  $m_A$  to be 200 MeV higher than the scalar diquark mass,  $m_A = 785$  MeV [17, 15]. The quark correlation affects the quark distributions through the diquark masses. The structure functions of the nucleon are written in terms of quark distribution functions, (3-2) and (3-3), e.g.  $F_2^p(x) = \frac{2}{3}xq^S(x) + \frac{1}{3}xq^A(x)$  and  $F_2^n(x) = \frac{1}{6}xq^S(x) + \frac{1}{2}xq^A(x)$ , where  $q^S(x)$  and  $q^A(x)$  are the quark distributions with the residual diquarks being the scalar and the axial-vector diquarks, respectively. We can write the spin dependent structure functions in terms of  $\delta^S(x)$  and  $\delta^A(x)$ .

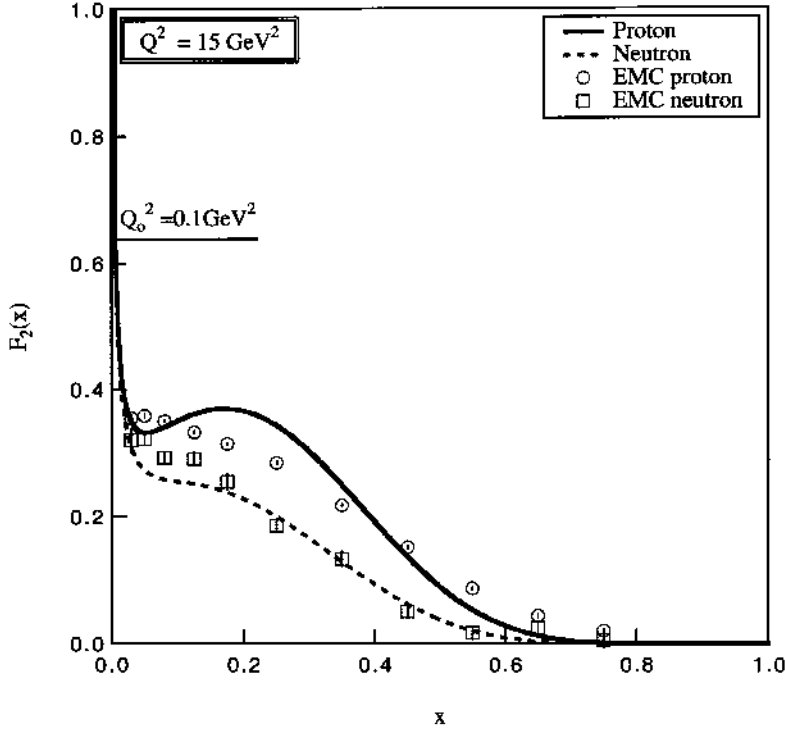


**Fig. 3.** Proton and neutron structure functions at  $Q^2 = 15 \text{ GeV}^2$ . The solid curve represents  $F_2^p(x)$ , and the dashed curve  $F_2^n(x)$ . Here, we use the low energy model scale  $Q_0^2 = 0.1 \text{ GeV}^2$ . The experimental data are taken from the EMC experiment [18].

We take the low energy model scale  $Q_0^2 = 0.1 \text{ GeV}^2$ , which is smaller than the one used in ref. [6]. Here, we use the first order Altarelli-Parisi equation [5] with  $\Lambda_{QCD} = 250 \text{ MeV}$ , in order to compare our result with experiment. The proton and the neutron structure functions  $F_2^p(x)$  and  $F_2^n(x)$  thus obtained at  $Q^2 = 15 \text{ GeV}^2$  are shown in Fig. 3 with experimental data [18], where we use  $m_A - m_S = 200 \text{ MeV}$ . Our result shows a reasonable agreement with experimental data. The second moments of the valence quarks are obtained as  $\langle xu_{val} \rangle = 0.273$ ,

$\langle xd_{val} \rangle = 0.106$  at  $Q^2 = 15 \text{ GeV}^2$ , and are consistent with experimental values; 0.275 and 0.116 [18]. Comparing our calculated results with the ones of the MIT bag model [19, 20] or the diquark spectator model [15], our structure functions are distributed over a much wider range of the Bjorken  $x$ . This result is the consequence of the strong diquark correlation.

We discuss here how the flavour structure of the structure function depends on the diquark correlation. The ratio  $F_2^n(x)/F_2^p(x)$  is shown in Fig. 4. Our result is in good agreement with experiment [18, 21, 22] with  $m_A - m_S = 200 \text{ MeV}$ . This is due to the dominance of  $u$ -quark distributions, namely  $q^S(x)$ , at large  $x$ , which is caused by the asymmetric momentum distributions of quarks and diquarks. In the middle  $x$  range,  $x \sim 0.4$ , the resulting ratio is close to  $2/3$ . We find that our calculated result is somewhat smaller than experiment at small  $x$ . The inclusion of sea quarks at the low energy scale enhances this ratio in the small  $x$  region, and may resolve this discrepancy. If we take the same values for the scalar and the axial-vector diquark masses, the ratio is close to  $2/3$ .

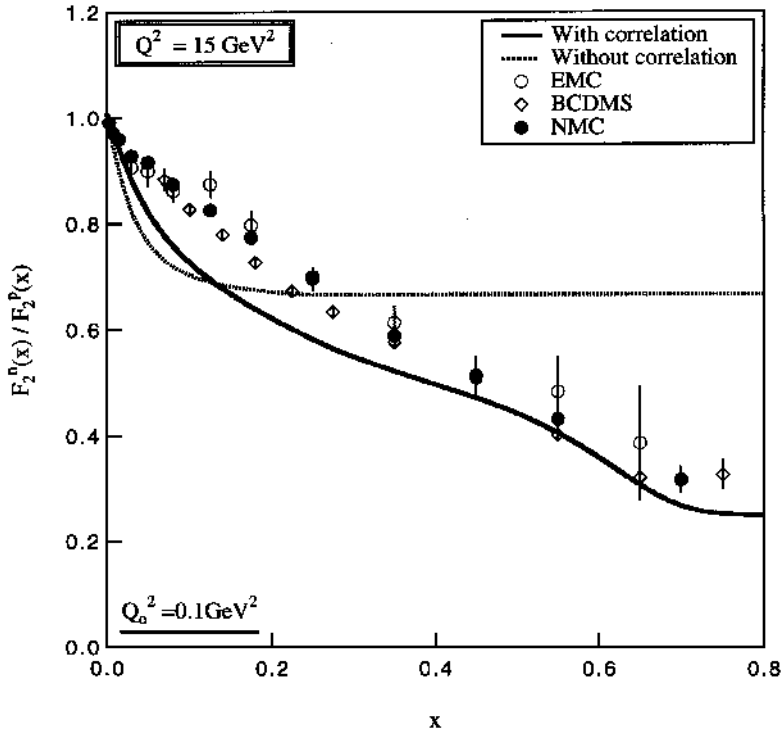


**Fig. 4.** Ratio of the nucleon structure functions  $F_2^n(x)/F_2^p(x)$  at  $Q^2 = 15 \text{ GeV}^2$  with  $m_A - m_S = 0$  (dotted), 200 MeV (solid) ( $Q_0^2 = 0.1 \text{ GeV}^2$ ). The experimental data are taken from ref. [18].

We next pay attention to the spin dependent structure function  $G_1^p(x)$  at  $Q^2 = 10 \text{ GeV}^2$ . The resulting structure functions yield a reasonable value for the Bjorken sum rule:

$$\int_0^1 dx [G_1^p(x) - G_1^n(x)] = \frac{1}{6} g_A (1 - \alpha_s/\pi).$$

We get 1.17 for the value of  $g_A$ , which is consistent with the experimental value 1.28. Further, we get the following value for the integral of  $G_1(x)$ ,  $\Gamma_p = \int_0^1 dx G_1^p(x) = 0.1249$ , which compares well with the recent data,  $0.126 \pm 0.006$  (SMC [11]). Ratios  $A_1^p = G_1^p(x)/F_2^p(x)$  and  $A_1^n$  are presented in Fig. 5. The result with the spin-0 quark correlation is depicted by the solid curve, and the dashed curve denotes the case without the correlation, which corresponds to the parton limit. The  $A_1^p$  calculated with the diquark correlation seems to provide a better result as the intermediate  $x$ , though it is not so apparent due to the experimental errors as compared with the spin independent case.

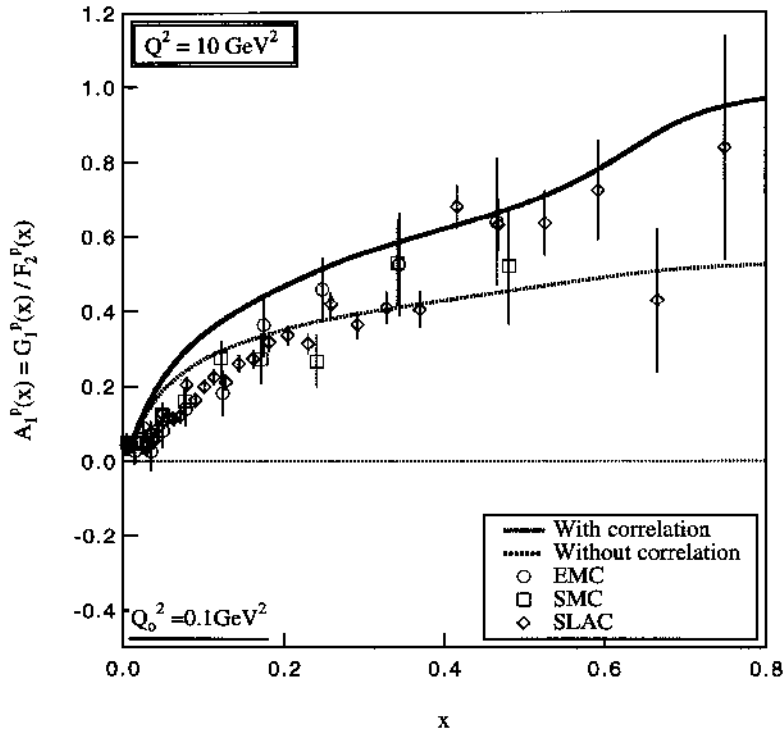


**Fig. 5.** Ratio of spin dependent to independent proton structure functions at  $Q^2 = 10 \text{ GeV}^2$  with SLAC E142 data. We use the model scale  $Q_0^2 = 0.1 \text{ GeV}^2$ . The solid curve depicts the result with the diquark correlation, and the dotted curve without the correlation.

Finally, we shall estimate the remaining distribution function  $h_1(x)$  in the study of the nucleon structure function. The steps in the calculation are the same as the one for  $f_1(x)$  and  $g_1(x)$  in the quark-diquark model. After some calculation, we find the following expression with the spectator diquark mass  $m_D$  [15]:

$$h_1^D(x) = \int_{p_E^2_{\min}}^{\infty} \frac{dp_E^2}{8\pi^2} \frac{|\phi_E|^2}{(p_E^2 + m^2)^2} [(p_E + m)^2 + 2(\mathbf{p}_\perp^E \cdot \mathbf{s})^2 - x(p_E^2 - M^2 - 2mM + m_D^2)], \quad (3-4)$$

where

$$\mathbf{p}_\perp^2 = -(1-x)p^2 + x(1-x)M^2 - xm_D^2.$$

We show the  $Q^2$  dependence of the chiral-odd distribution functions in Fig. 6. For simplicity, we use the first order Altarelli–Parisi equation [5] with  $\Lambda_{QCD} = 250$  MeV and the low energy model scale  $Q_0^2 = 0.1$  GeV<sup>2</sup>. As  $Q^2$  increases, the peak of the distribution function shifts to small  $x$ , and its absolute magnitude becomes small. Note that the absolute magnitude of the  $u$  quark distribution is considerably larger than the  $d$  quark, because the scalar diquark is dominant in the proton.

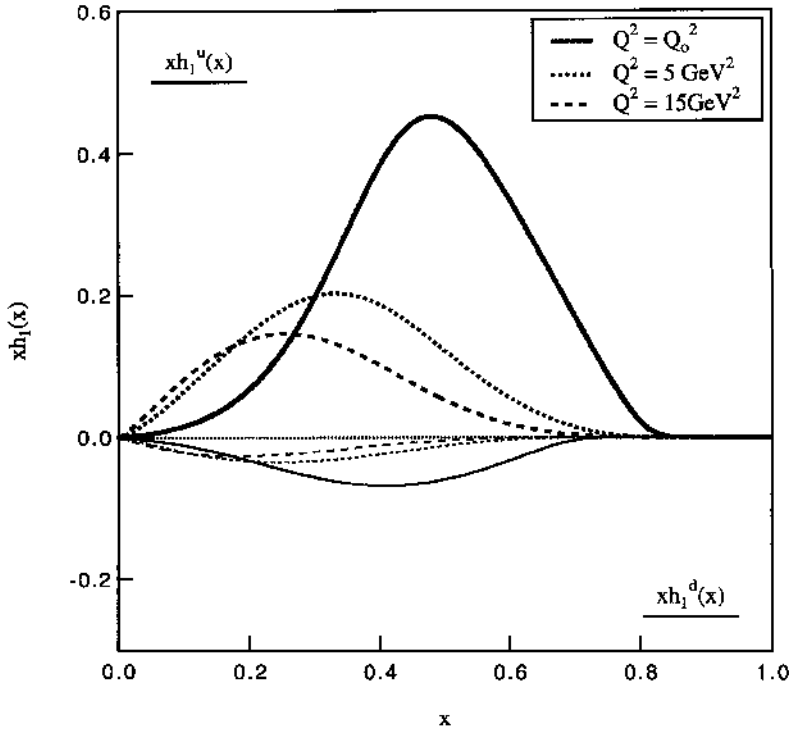


**Fig. 6.** Chiral-odd distribution functions of the valence quark at the low energy scale  $Q^2 = Q_0^2$ , and  $Q^2 = 5$  and  $15$  GeV<sup>2</sup>. The  $u$  quark distributions are depicted by thick curves and  $d$  quark distributions by thin curves, respectively. The solid curves are at  $Q^2 = Q_0^2$ , the dotted curves at  $Q^2 = 5$  GeV<sup>2</sup> and the dashed curves at  $Q^2 = 15$  GeV<sup>2</sup>.

We calculate also the integrated values for the distributions. The *tensor charge*  $\delta q$  and *axial charge*  $\Delta\Sigma$  are expressed in terms of  $h_1^q(x)$  and  $g_1^q(x)$ , respectively.

The tensor charge corresponds to the transversity, which represents the fraction of the transverse spin of the quarks. The expression for the tensor charge in terms of  $h_1^q(x)$  and  $h_1^{\bar{q}}(x)$  is  $\delta q \equiv \int_0^1 dx [h_1^q(x) - h_1^{\bar{q}}(x)]$ . Our result for the tensor charge is  $\delta q = 0.90$ . This result is reasonably consistent with recent estimates of the tensor charge with the MIT bag model [23] of  $\delta q = 0.88$ . On the other hand, the axial charge,  $\Delta\Sigma \equiv \int_0^1 dx [g_1^q(x) - g_1^{\bar{q}}(x)]$ , which corresponds to the fraction of the spin of the nucleon carried by the quarks comes out to be  $\Delta\Sigma = 0.299$ . This is smaller than the recent estimates with the MIT bag model of  $\Delta\Sigma = 0.38$ .

#### 4. Summary and Conclusion

We have studied the structure functions of hadrons with the low energy effective theory of QCD. We have tried to clarify a link between the low energy effective theory, where non-perturbative dynamics is essential, and the high energy deep inelastic experiment, where the perturbative description is possible for its momentum dependence.

We have used the NJL model to obtain the meson structure functions. Our results are in reasonable agreement with experimental data, except for the large  $x$  region. In this region, the struck quark carries a large momentum  $> 1$  GeV, and the NJL model is not designed for the momentum  $p^2 > \Lambda^2 \sim 1$  GeV<sup>2</sup>. Generally, the phenomenological quark wave functions, e.g. the Isgur–Karl model (harmonic oscillator type) or the MIT bag model, do not include such high momentum components. We have to improve the behaviour of the structure function at large  $x$ , by taking into account the quark correlation in the high momentum region. Higher twist contributions are also expected to change the shape of the distribution function at large  $x$ . On the other hand, the kaon structure function provides valuable data on the strange sector. As we have discussed for the kaon, the valence strange quark may carry a larger momentum fraction than the up or down quark in the kaon. Comparing the  $u$ -quark distribution in the kaon  $u_K(x)$  with that in the pion  $u_\pi(x)$ , the NJL model calculation indicates the dominance of  $u_\pi(x)$  at the large  $x$ , and is consistent with the available data. This is due to the strong quark correlation in the pion, namely, the binding energy of the  $u$ -quark in the pion is larger than that in the kaon.

We have studied the distribution functions of the nucleon based on the phenomenological quark–diquark model. This model reproduces the asymmetric momentum distributions in the nucleon. The non-perturbative effects in this model are found in the quark distribution function. We have paid special attention to the ratio of the structure function, in which we can see clearly the non-perturbative effect on the structure function. The neutron to proton structure function ratio,  $F_2^n(x)/F_2^p(x)$ , shows good agreement with the available DIS data. Our result indicates that the quark correlation, especially in the scalar channel, is important to understand the DIS data. We have also calculated the spin dependent structure function, and our calculation reproduces the experimental data of  $G_1^p(x)/F_1^p(x)$ .

In our studies of the structure functions of hadrons, the meson and the nucleon, within the QCD effective model, we have compared the model calculations with the experiments. We can see how the non-perturbative dynamics of the effective theory is reflected in the deep inelastic scattering phenomena. It is very important to recognize that non-perturbative dynamics at the low energy scale affect the high energy phenomena.

## References

- [1] T. Shigetani, K. Suzuki and H. Toki, Nucl. Phys. **A579** (1994) 413.
- [2] See e.g. R. G. Roberts, 'The Structure of the Proton' (Cambridge Univ. Press, 1990).
- [3] P. V. Landshoff, J. C. Polkinghorne and R. D. Short, Nucl. Phys. **B28** (1971) 225.
- [4] V. Bernard, R. L. Jaffe and U.-G. Meissner, Nucl. Phys. **B308** (1988) 753.
- [5] G. Altarelli and G. Parisi, Nucl. Phys. **B126** (1977) 298.
- [6] M. Glück, E. Reya and A. Vogt, Z. Phys. **C53** (1992) 651.
- [7] P. J. Sutton, A. D. Martin, R. G. Roberts and W. J. Stirling, Phys. Rev. **D45** (1992) 2349.
- [8] J. Badier *et al.*, Phys. Lett. **B93** (1980) 354.
- [9] J. Ashman *et al.* (EMC), Phys. Lett. **B206** (1988) 364; Nucl. Phys. **B328** (1989) 1.
- [10] D. Adams *et al.* (SMC), Phys. Lett. **B329** (1994) 399.
- [11] P. Anthony *et al.*, SLAC E-143 Preprint (1994).
- [12] R. L. Jaffe and X. Ji, Nucl. Phys. **B375** (1992) 527.
- [13] A. Donnachie and P. V. Landshoff, Phys. Lett. **B95** (1980) 437.
- [14] C. J. Burden, R. T. Cahill and J. Praschifka, Aust. J. Phys. **42** (1989) 147;  
A. Buck, R. Alkofer and H. Reinhardt, Phys. Lett. **B286** (1992) 29;  
N. Ishii, W. Bentz and K. Yazaki, Phys. Lett. **B301** (1993) 165.
- [15] H. Meyer and P. J. Mulders, Nucl. Phys. **A528** (1991) 589.
- [16] J. H. Donoghue and K. S. Sateesh, Phys. Rev. **D38** (1988) 360.
- [17] F. E. Close and A. W. Thomas, Phys. Lett. **B212** (1988) 227.
- [18] J. J. Aubert *et al.* (EMC), Nucl. Phys. **B293** (1987) 740.
- [19] C. J. Benesh and G. A. Miller, Phys. Rev. **D36** (1987) 1344.
- [20] A. W. Schreiber, A. I. Signal and A. W. Thomas, Phys. Rev. **D44** (1991) 2653, and references therein.
- [21] P. Amaudruz *et al.* (NMC), Phys. Rev. Lett. **66** (1991) 2716; Nucl. Phys. **B371** (1992) 3; Phys. Rev. **D50** (1994) R1.
- [22] A. C. Benvenuti *et al.* (BCDMS Collaboration), Phys. Lett. **B237** (1990) 599.
- [23] J. Soffer, Phys. Rev. Lett. **74** (1995) 1292.